Extracting oil palm crown from WorldView-2 satellite image

A Korom[1,4], M-H Phua[2], Y Hirata[3] and T Matsuura[3]
[1] Faculty of Plantation and Agrotechnology, University Technology MARA (Sabah), 88997 Kota Kinabalu, Sabah, MALAYSIA
[2] School of International Tropical Forestry, University Malaysia Sabah, Jalan UMS, 88400 Kota Kinabalu, Sabah, MALAYSIA
[3] FFPRI, Matsunosoto 1, Tsukuba, Ibaraki, 305-8687, JAPAN

E-mail: alexi502@sabah.uitm.edu.my

Abstract. Oil palm (OP) is the most commercial crop in Malaysia. Estimating the crowns is important for biomass estimation from high resolution satellite (HRS) image. This study examined extraction of individual OP crown from a WorldView-2 image using twofold algorithms, i.e., masking of Non-OP pixels and detection of individual OP crown based on the watershed segmentation of greyscale images. The study site was located in Beluran district, central Sabah, where matured OPs with the age ranging from 15 to 25 years old have been planted. We examined two compound vegetation indices of (NDVI+1)*DVI and NDII for masking non-OP crown areas. Using kappa statistics, an optimal threshold value was set with the highest accuracy at 90.6% for differentiating OP crown areas from Non-OP areas. After the watershed segmentation of OP crown areas with additional post-procedures, about 77% of individual OP crowns were successfully detected in comparison to the manual based delineation. Shape and location of each crown segment was then assessed based on a modified version of the goodness measures of Möller et al which was 0.3, indicating an acceptable CSGM (*combined segmentation goodness measures*) agreements between the automated and manually delineated crowns (perfect case is '1').

1. Introduction

High resolution satellite images have been increasingly available to resource managers. Beside of its photographic details, the images have been analysed based on geographic object-based image analysis (GEOBIA) for many important applications such as landscape mapping, riparian ecological studies, forest canopy gap studies, individual tree delineation, tree species identification and many more owing to technological enhancement, satellite sensor refinement as well as availabilities of commercial softwares [1-3]. This field evolves fast in recent years starting 1990s, involving many fields of research replacing pixel-based technique at macro and micro levels. However, there has been a lack of emphasize on extraction of tree individual OP crown in tropical region. Oil palm plantation has been seen as the driver of deforestation of tropical forest which contributes to carbon sink.

A crown object can be detected as a group of homogeneous vegetation pixels in any HRS images such as QuickBird and IKONOS. WorldView-2 (WV-2) has the advantage of more chlorophyll-sensitive bands, e.g., red edge (RE), near-infrared 1 (NIR) and 2 (NIR2), beside of visible bands. Ideally, an individual tree top appears as the brightest pixels in multispectral imagery and can be easily masked (figure 1a). Oil palm appears differently due to its morphological arrangement of leaves component (figure 1b) that make it difficult to segment individually. With the WV-2's chlorophyll-sensitive bands, we developed an approach that uses vegetation indices to improve oil palm crown segmentation. However in GEOBIA, it is possible to analyze both pixel spectral and object information such as crown size, shape, texture, entropy and its occurrences relative to other object

[4] To whom any correspondence should be addressed

which are useful for discovering relationship with tree biomass [4-6]. Obviously here, the crown extraction is very important as primary base work which is the main objective of this paper.

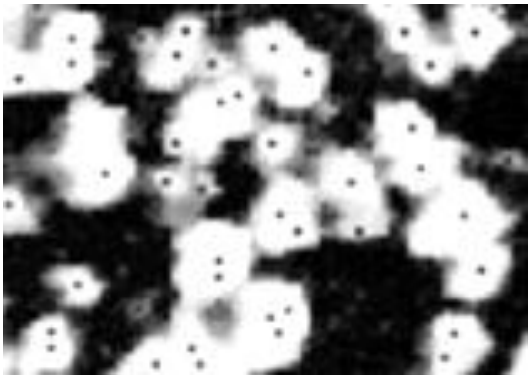

a) Ordinal tree: Image from airborne multispectral data. Source: [7]. Dark dots within white pixels group indicate the summits of tree crowns.

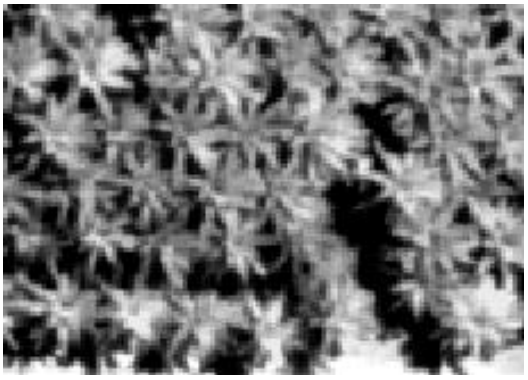

b) Oil palm: Image from WorldView-2 (panchromatic)

Figure 1: Different appearances between ordinal trees (a) and oil palms (b) in satellite imagery

2. Study area and WorldView-2 imagery

The study area is located in Beluran district which is about 120 km to the west of Sandakan city, the second largest city in Sabah, Malaysia. This oil palm plantation consists of 34 blocks which range from 25 to 97 ha area. Oil palms in this area are matured, i.e., from 15 to 25 years old. Terrain in this area is undulating with elevation ranges from 60 to 138 meters above mean sea level. WV-2 satellite image for this area was captured on May 10, 2010 over an area of upper left (5°32'30" N, 117°15'45" E) to lower right (5°29'30" N, 117°19'05" E) covering 25 square km. The image was radiometrically corrected and geo-rectified using a DEM of SRTM 30 meter. About 10% of the image area was covered by clouds and their shadows. WV-2 consists of two groups of bands; panchromatic (0.46m) and multispectral (1.84m). Data set uses in this analysis was pan-sharpened which was better for object identification [8].

3. Data collection

In total, 20 circular sampling plots with a radius of 15 m were measured and each plot was selected based on line transect approach. Field inventory was conducted from Oct 2011 to Jul 2012. The palm ages were 15, 18, 24 and 25 years. Each plot contained from eight to thirteen palms. Centre location of a plot was taken using a handheld GPS. Positions of trees within a plot were measured with direction and distance from the centre point. Based on the pair-match identification between uncorrected fixed point and manually detected trees, deviated errors were from 2.5 to 9 meters.

4. OP class thresholding and Kappa analysis

Two major tasks, OP versus Non-OP classification and watershed segmentation, were implied before the crown segment can be extracted out from the image. Because it is difficult to directly segment the oil palm crown at individual level due to its morphological appearances on satellite images, here vegetation indices (Table 1) were used to help the segmentation through improving an object visuals [9] and segregating oil palm and non oil palm objects [10].

Table 1. Vegetation indices

Vegetation Index	**Formula**	**Range**	**Reference**
Normalized Difference Vegetation Index	$NDVI=\frac{NIR - R}{NIR + R}$	-1 to +1	[11]
Normalized Difference Infrared Index	$NDII=\frac{NIR - RE}{NIR + RE}$	-1 to +1	[12]
Differential Vegetation Index	$DVI=NIR - R$	∞	[13]

Note: R (red, 630-690 nm), RE (red edge, 705-745 nm) and NIR (near-infrared, 770-895nm)

Threshold values were set strategically unto two compound vegetation indices; (NDVI + 1)DVI and NDII. Each index separates pixels at the midpoint between two object classes; lower values represent no vegetation whereas higher values represent vegetation. Kappa coefficient (κ) was used to select a threshold value around the midpoint and the threshold value with the highest κ was selected. It normally does not take more than ten trials for Kappa calculations to reach the converged point. The thresholding processes in detail were shown in table A1 and A2 in appendices. Finally, they were combined to produce a better class map of OP versus Non-OP as shown in figure 2.

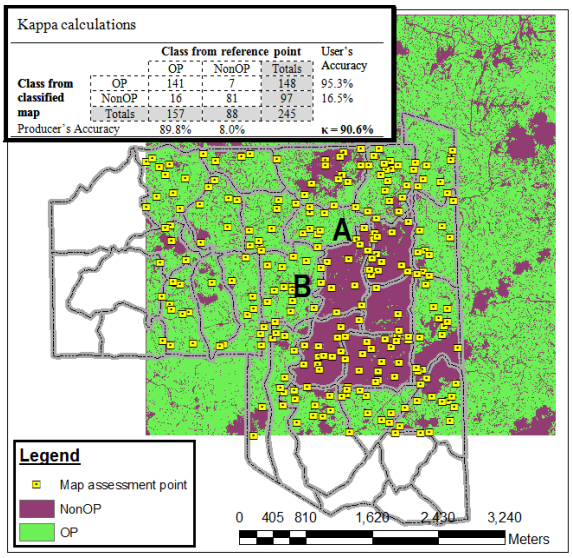

Figure 2: Final class map of OP versus Non-OP together with Kappa analysis for map accuracy assessment. Total of 254 sample points were randomly assigned and validated based on visual observation at close range of image

5. OP individual segmentation

Non-OP class masking was applied unto the original image. Afterwards post-segment filtering was used to clean up the defect segments (segments with anomalous shape size and asymmetry). Two groups of factors, i.e., shape and spectral (Table 2), were used to filter out the defect segments. Quality of segmentation was further assessed using modified Möller measures listed in table B1 in the appendix. For shape evaluation, reference segments of individual OP crowns were digitized at the selected plots and matched accordingly to its respective pair of extracted segment. Those segments were evaluated based on their shape and position (indicated by *Combined Segment Goodness Measures* or CSGM in table B.1 at appendix) which '1' represents the best and '0' is vice versa.

Table 2. Shape and spectral factors for post processing of segmentation

Criteria	Threshold	Formula
Area	Less than 30 m^2 OR greater than 120 m^2	*No. of pixel* × 0.25m^2/*pixel*
Perimeter-area ratio	Less than 0.3	$ratio = \frac{P}{A}$
Compactness index	Less than 1.9	$CI = \frac{P}{2\sqrt{\pi \emptyset}}$
Red edge	Greater than 50	

6. Results and discussion

6.1 Crown extraction assessment

Assessment on class map in figure 2 revealed that Kappa accuracy was very high (90.6%). Usually several calculations are needed to determine the best threshold but it is sometimes possible to obtain the best threshold value at the first trial. After the post segmentation processing, about 77% of the total tree crown segments were successfully delineated. Unfit segments were further removed because they do not represent crown areas in terms of their size and shape.

We found that vegetation index greatly enhanced the OP crowns which make the detection much easier. Palm crown were detected based on the presence of higher chlorophyll content. However sometimes, a crown can be partitioned into smaller segments due to the patchy distributions of leave biomass. This crown subdivision problem causes more polygons being extracted as shown in table 3. Detailed analysis of crowns at different ages was over the scope of this study.

Table 3. Assessment of OP crown extraction performance

Block name	Age (year)	No. of trees	Planned planting area (ha)	Planted area (ha)	Classified area (ha)		No. of extracted polygons	Percentage of over extract
					OP	Non-OP		
A	24	3655	50	47	35.02	5.93	4446	21.6%
B	15	5616	50	47	54.60	10.23	6890	22.7%

Note: Information regarding each block such as age, number of trees per block and indicated areas were from oil palm plantation management. Out of 34 blocks, only two were free of crowd and shadow and can be used for comparison.

6.2 Möller's shape and location based goodness measures

Task to extract individual oil palm crown is challenging due to their morphological appearances. Segmentation using only RGB bands often resulted in outrageous oversegmentation. Our approach managed to achieve 0.3 of goodness index (CSGM) for shape and location of overall segments which indicated an acceptable performance (perfect segmentation is "1"). Note that the manually delineated segments were not the real crown plan-shapes but they reasonably serve as the basis to compare. Figure 3 shows the extracted individual oil palm crowns. Mismatched boundary lines between the manual and automated extractions (see figure 3, left side) demonstrated the acceptable quality of our segmentation using the watershed technique.

7. Conclusions

Potential of WV-2 has been explored and assessed to extract individual oil palm crowns. Although it morphologically appears scattered and patchy, individual oil palm crowns can be delineated by masking the non-OP areas using combined vegetation indices before segmentation. Post segment processes are required to reduce commission and omission errors. Crown shape and dimension extracted from high resolution satellite image may correlate with other vegetation parameters, which have not been satisfactorily investigated.

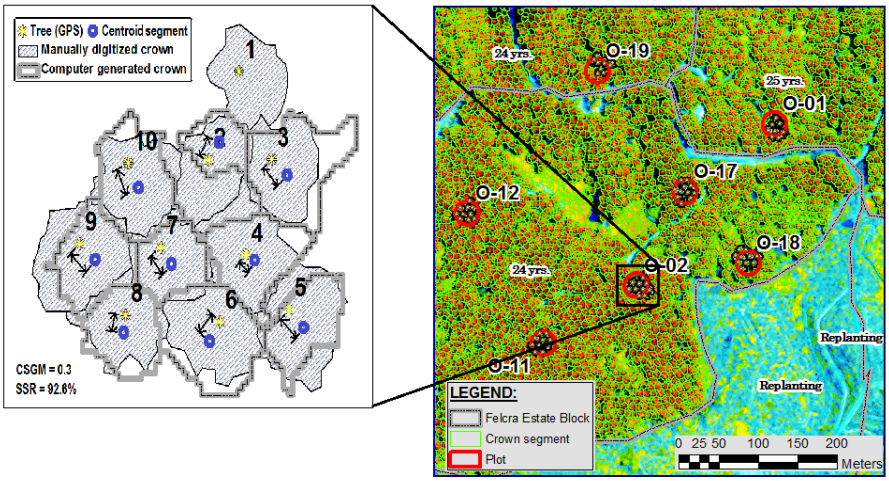

Figure 3: Crown shape and location assessment

8. Appendices

Table A1: Kappa calculations using midpoint threshold values of a compound vegetation index: (NDVI + 1)DVI

Midpoint	Threshold value	Kappa coefficient	Overall accuracy	User's accuracy		Producer's accuracy	
				OP	Non OP	OP	Non OP
Minimum	0	0.26	0.60	0.83	0.53	0.48	0.18
4th	87	0.64	0.85	0.81	0.02	0.99	0.41
3rd	174	0.69	0.87	0.85	0.10	0.96	0.30
*6th	196	0.73	0.88	0.88	0.11	0.95	0.24
7th	207	0.72	0.87	0.88	0.14	0.93	0.23
5th	218	0.71	0.87	0.88	0.15	0.92	0.23
4th	261	0.67	0.84	0.89	0.23	0.86	0.18
5th	305	0.68	0.84	0.92	0.26	0.83	0.13
2nd	348	0.61	0.81	0.92	0.32	0.77	0.13
3rd	522	0.31	0.61	0.96	0.52	0.41	0.03
1st	696	0.03	0.39	0.90	0.63	0.06	0.01
2nd	1044	0	0.36	NA	0.64	0.00	0.00
Maximum	1392	0	0.36	NA	0.64	0.00	0.00

Note: * Best threshold, NA not available

Table A2: Kappa calculations using midpoint threshold values of a vegetation index: NDII

Midpoint	Threshold value	Kappa coefficient	Overall accuracy	User's accuracy		Producer's accuracy	
				OP	Non OP	OP	Non OP
Minimum	-0.351	0	0.36	NA	0.64	0	0
3rd	-0.048	0.64	0.85	0.81	0	1.00	0.42
2nd	-0.149	0.04	0.65	0.65	0	1.00	0.97
*1st	0.054	0.83	0.92	0.93	0.09	0.95	0.13
5th	0.079	0.77	0.89	0.94	0.18	0.89	0.10
4th	0.104	0.74	0.87	0.96	0.24	0.83	0.06
3rd	0.155	0.49	0.73	0.99	0.43	0.58	0.01
2nd	0.256	0.06	0.53	0.07	0	1.00	0.49
Maximum	0.458	0	0.64	0.64	NA	1.00	1.00

Note: * Best threshold, NA not available

Table B1: Möller segment assessment formula [14,15]

Goodness measures	Individual pair	Global
Oversegmentation	$OSeg_{ij}=1-\frac{area(a_i \cap b_j)}{area(a_i)}$, $b_j \in B_i^*$	$GOSeg=\sqrt{\frac{\sum_{l=1}^{k} OSeg_{ij,l}^2}{(k-1)}}$
Undersegmentation	$USeg_{ij}=1-\frac{area(a_i \cap b_j)}{area(b_j)}$, $b_j \in B_i^*$	$GUSeg=\sqrt{\frac{\sum_{l=1}^{k} USeg_{ij,l}^2}{(k-1)}}$
Gap centroid dislocation	$\lvert dist_{a_i-b_j}\rvert=\sqrt{(x_i-x_j)^2+(y_i-y_j)^2}$ and **Relative position,** $RP_{ij}=\frac{dist_{ij}}{dist_{ijMax}}$	$GapD=\sqrt{\frac{\sum_{l=1}^{k} RP_{ij,l}^2}{(k-1)}}$
Combined segmentation		$CSGM=\sqrt{\frac{GOSeg^2+GUSeg^2+GapD^2}{3}}$

Note: Where a_i = manual digitized segment with *i* no. of object,
b_j = computer generated segment with *j* no. of object,
B_i^* = union of all possibilities matching cases, and
$area(a_i \cap b_j)$ = coincide area between a_i and b_j

9. References

[1] Addink E A, Van Coillie F M B and De Jong S M 2012 *Int. J. of Appl. Earth Observation and Geoinformation* **15** 1-6
[2] Blaschke T 2010 *ISPRS J. of Photogram. and Rem. Sensing* **65** 2-16
[3] Hay G J and Blaschke T 2010 *Photogram. Engineering and Rem. Sensing,* **76** 121-122
[4] Lu D 2005 *Int. J. of Rem. Sensing* **26** 2509-2525
[5] Phua M H and Saito H 2003 *Canadian J. of Rem. Sensing* **29** 429-440
[6] Hirata Y, Tabuchi R, Patanaponpaiboon P, Poungparn S, Yoneda R and Fujioka Y 2013 *J. of Forest Research* 1-8
[7] Wulder M, Niemann K O, and Goodenough D G 2000 *Rem. Sens. of Environment* **73** 103-114
[8] Ardila J P, Tolpekin V A, Bijker W and Stein A 2011 *ISPRS J. of Photogrammetry and Remote Sensing* **66** 762-775
[9] Peña-Barragán J M, Ngugi M K, Plant R E and Six J 2011 *Remote Sensing of Environment* **115** 1301-1316
[10] Santoso H, Gunawan T, Jatmiko R, Darmosarkoro W and Minasny B 2011 *Precision Agriculture* **12** 233-248
[11] Rouse J W, Haas R H, Schell J A and Deering D W 1974 *Third Earth Resources Technology Satellite-1 ERTS Symposium* 301-319.
[12] Hardisky M A, Klemas V and Smart R M 1983 *Photogrammetric Engineering and Remote Sensing* **49** 77-83
[13] Richardson A J and Everitt J H 1992 *Geocarto International* **7** 63-69
[14] Möller M, Lymburner L and Volk M 2007 *Int. J. of Applied Earth Observation and Geoinformation* **9** 311-321
[15] Clinton N, Holt A, Scarborough J, Yan L and Gong P 2010 *Photogrammetric Engineering and Remote Sensing* **76** 289-299